www.czasopisma.pan.pl PAN POLSKA AKADEMIA NAUK www.journals.pan.pl

Arch. Metall. Mater. **65** (2020), 2, 975-982

DOI: 10.24425/amm.2020.132846

D. BRZEZIŃSKA[1*]

PROPERTIES OF $Pb_{1-x}Ba_x(Zr_{1-y}Ti_y)_{1-z}Sn_zO_3$ ($x = 0.03$, $y = 0.02$, $z = 0 \div 0.08$) CERAMICS

This paper presents the results of obtaining and investigations of $Pb_{1-x}Ba_x(Zr_{1-y}Ti_y)_{1-z}Sn_zO_3$ (PBZTS) ceramics with constant $x = 0.03$ and $y = 0.02$, and variable $z = 0$, 0.04, 0.06 and 0.08 (abbreviations of the samples were following PBZTS0, PBZTS4, PBZTS6, PBZTS8, respectively). The investigated compositions are close to rhombohedral-orthorhombic morphotropic phase boundary. The ceramic samples have been obtained by conventional ceramic technology from simple oxides PbO, ZrO_2, TiO_2, SnO_2 and barium carbonate $BaCO_3$. The ceramic powders, after calcination, have been pressed into discs and sintered using free sintering (FS) method. For samples obtained in such a way, the dielectric properties at various frequencies and electrical conductivity have been investigated. The increase of Sn content orders the microstructure of ceramics, and as a result the improvement of the dielectric properties of ceramic samples can be obtained.

Keywords: PBZT and PBZTS ceramics, phase transitions, dielectric properties, electrical conductivity

1. Introduction

PZT-type ceramic materials have been researched for many years. Based on PZT ceramics, new materials with interesting application properties are produced [1-2]. The investigated $Pb_{1-x}Ba_x(Zr_{1-y}Ti_y)_{1-z}Sn_zO_3$ (PBZTS) is based on the well-known solid solution $Pb_{1-x}Ba_xZr_{1-y}Ti_yO_3$ (PBZT – which is widely described in work [3]) and belongs to lead containing perovskite-type oxides which are very important for practical applications (for example electromechanical transducers [4], capacitors [5] etc.). The technology of obtaining PBZT was first described in [6], whereas the phase diagram of this solid solution was presented in reference [7]. At room temperature, for $x = 0.03$ and $y = 0.02$, PBZT should exhibit the orthorhombic symmetry of elementary cells and antiferroelectric properties (see Fig. 1 based on works [7-8]). Examples of the investigations of properties of PBZT ceramics are presented in works [9-10]. In work [11], $Pb_{0.975}Ba_{0.025}Zr_{1-y}Ti_yO_3$ ceramics were prepared using solid state reaction method with $0 \leq y \leq 1$. The sintering temperature was 1200°C for 3 h. It was found that the structural phase indexed in the orthorhombic phase for $y = 0$ sample. The tetragonal phase was detected in $0.25 \leq y \leq 1$ ceramic samples.

The results of obtaining and investigations of basic dielectric properties of $Pb_{1-x}Ba_x(Zr_{1-y}Ti_y)_{1-z}Sn_zO_3$ ceramics were presented in work [12]. PBZTS ceramics is an interesting material due to its ferroelectric, antiferroelectric or relaxor properties depending on the designed composition and changing temperature. The introduction of Sn^{4+} ion into B-position of the perovskite

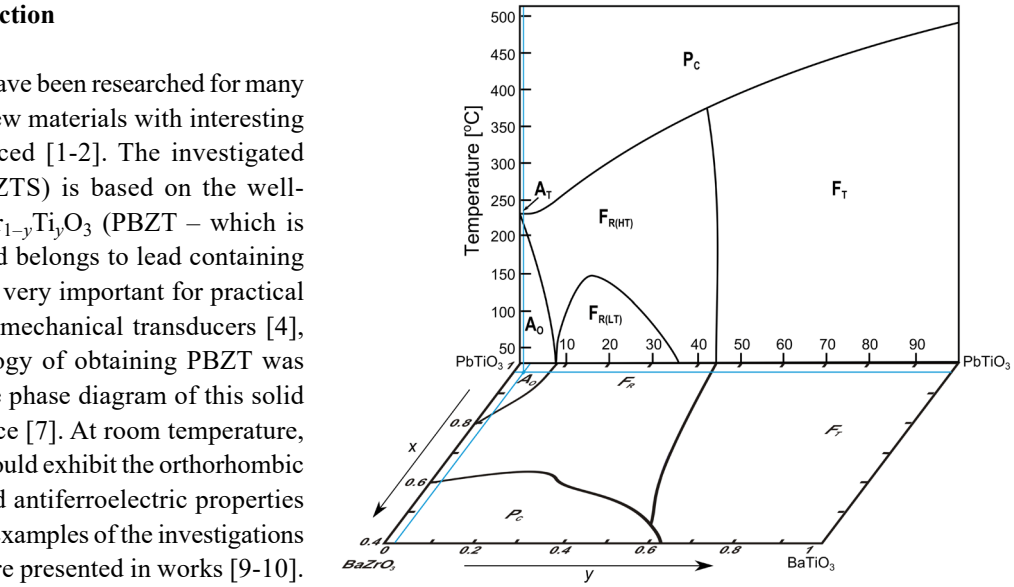

Fig. 1. The starting composition (without Sn) marked on the PZT phase diagram and PBZT phase diagram at room temperature from work [7-8]

[1] UNIVERSITY OF SILESIA IN KATOWICE, INSTITUTE OF MATERIALS ENGINEERING, FACULTY OF SCIENCE AND TECHNOLOGY, 75 PUŁKU PIECHOTY 1A, 41-500 CHORZÓW, POLAND

* Corresponding author: dagmara.brzezinska@us.edu.pl

structure leads to the change of the electrophysical parameters relevant to applications in devices such as, for instance, actuators that transform energy and pulse capacitors etc. The addition of SnO_2 to the base PBZT composition gives the possibility of influencing the parameters relevant for practical applications in the areas of micromechatronics and microelectronics [13]. In work [12], it has been stated that the increase of the content of Sn reduces the size of the unit cell. This may be connected with the fact that the ionic radius of Sn^{4+} (r_i = 0.074 nm) is smaller than the Zr^{4+} (r_i = 0.087 nm). Radius of titanium ion (r_i = 0.061 nm) is smaller than the Sn ion, however in the investigated samples the amount of titanium is in a small. Also other compositions of PBZST were investigated, for instance, the composition $Pb_{1-x}Ba_x(Zr_{1-y}Ti_y)_{1-z}Sn_zO_3$ with $x = 0.25$, $y = 0.35$ and $z = 0.00$, 0.02, 0.04, 0.08, 0.10 [14-15]. There is relatively little data on such solid solutions, despite of the fact that the properties thereof are very interesting [16].

For the samples obtained in [12], the following have been presented: results of investigations of SEM images of fractured $Pb_{0.97}Ba_{0.03}(Zr_{0.98}Ti_{0.02})_{1-z}Sn_zO_3$ samples, the chemical composition using EDS technique, X-ray diffraction patterns, temperature dependencies of $\varepsilon'(T)$ and $\tan\delta(T)$, however only using frequency 1 kHz, and also *P-E* hysteresis loops at various temperatures. Normal ferroelectric *P-E* hysteresis loops were observed within the temperature range of 100-150°C, even for $Pb_{1-x}Ba_x(Zr_{1-y}Ti_y)_{1-z}Sn_zO_3$ (PBZTS) ceramics with $x = 0.03$, $y = 0.02$ and $z = 0$. Measurements of hysteresis loops at lower temperatures, including room temperature, were not possible due to the very large coercion field. It shall also be remembered that this composition is close to the boundary between orthorhombic and rhombohedral phases, and this boundary can significantly depend on temperature [12].

The present paper includes the results of the measurements of $\varepsilon'(T)$ and $\tan\delta(T)$, tested in a wider frequency range from 0.5 kHz to 1 MHz, as well as the results of measurements of DC and AC electrical conductivity.

2. Experimental

The technology of obtaining of the investigated PBZTS ceramics used in this paper is similar to the technology described in [12]. The substrates of all compositions were dried at 150°C to evaporate water (moisture) and then weighed according to the stoichiometric ratio. In order to avoid lead deficiency arising during the high temperature sintering process, a 5% surplus of PbO was added. Final sintering was carried out under conditions T_s = 1250°C/t_s = 4 h (5°C/min), using PbO+ZrO_2 mixed powders (30/70) as a ballast, as well as with sticking the crucible to minimize the loss of lead oxide. For dielectric and electromechanical investigations, the last step of technology was the application of silver paste electrodes on both surfaces of the samples. The samples with applied silver paste were burned in the furnace at 850°C/15 min. The compositions of the obtained PBZTS ceramic samples are presented in Table 1.

TABLE 1

The compositions of the obtained PBZTS ceramic samples

Abbrev.	Basic composition mark	z (Sn content)
PBZTS0	$Pb_{0.97}Ba_{0.03}(Zr_{0.98}Ti_{0.02})O_3$	0
PBZTS4	$Pb_{0.97}Ba_{0.03}(Zr_{0.98}Ti_{0.02})_{0.96}Sn_{0.04}O_3$	0.04
PBZTS6	$Pb_{0.97}Ba_{0.03}(Zr_{0.98}Ti_{0.02})_{0.94}Sn_{0.06}O_3$	0.06
PBZTS8	$Pb_{0.97}Ba_{0.03}(Zr_{0.98}Ti_{0.02})_{0.92}Sn_{0.08}O_3$	0.08

Similarly as in work [12], a HITACHI S-4700SEM scanning electron microscope was used to investigate the microstructure of fractured samples. Earlier EDS studies revealed that the chemical composition after sintering was close to the assumed one. The presence of foreign elements or impurities was also excluded.

The dielectric measurements were performed using an LCR meter (QuadTech, Inc., 1920 Precision LCR meter, Maynard, MA, USA) during the heating cycle (in temperature range from 20°C to 450°C), at frequencies of the measurement field from 0.5 kHz to 1.0 MHz.

DC electrical conductivity has been measured using an electrometer by Keithley Instruments, Inc., 6517B, Cleveland, OH, USA, within the temperature range from 20°C to 450°C.

AC electrical conductivity has been calculated from the dielectric measurements presented according the formula:

$$\sigma_{ac} = \omega \cdot \varepsilon_0 \cdot \varepsilon' \cdot \tan\delta \tag{1}$$

where ω is angular frequency, ε_0 is vacuum permittivity, ε' is a real part of relative permittivity and $\tan\delta$ is the loss tangent.

The relationship between AC conductivity and frequency are well described by the universal Jonscher's power law (UDR) [17-18]:

$$\sigma_{ac}(\omega) = A\omega^s \tag{2}$$

where $\sigma_{ac}(\omega)$ is the AC conductivity, ω is the angular frequency, s is the frequency exponent – the depending on temperature parameter (i.e. frequency independent).

3. Results and discussion

The SEM microstructures of the ceramic samples are presented in Fig. 2. The analysis of the microstructure reveals that the grains are characterized by irregular shapes. In all of the compositions the mechanism of cracking on the grain boundary is observed, as the dominant mechanism with a small share of the cracking mechanism through the grain. The samples have visible porosity. In the microstructure without Sn there is a large heterogeneity of the size of grains, there are large and fine grains. Introduction to the base composition of Sn admixture organizes domain structure (but without a clear tendency to influence the amount of Sn on surface morphology). For PBZTS8 ceramics, there is the greatest homogeneity of grain size. Sn addition causes the boundaries of grains to lose a pronounced appearance, and the grain between boundaries is not sharp. Microstructural

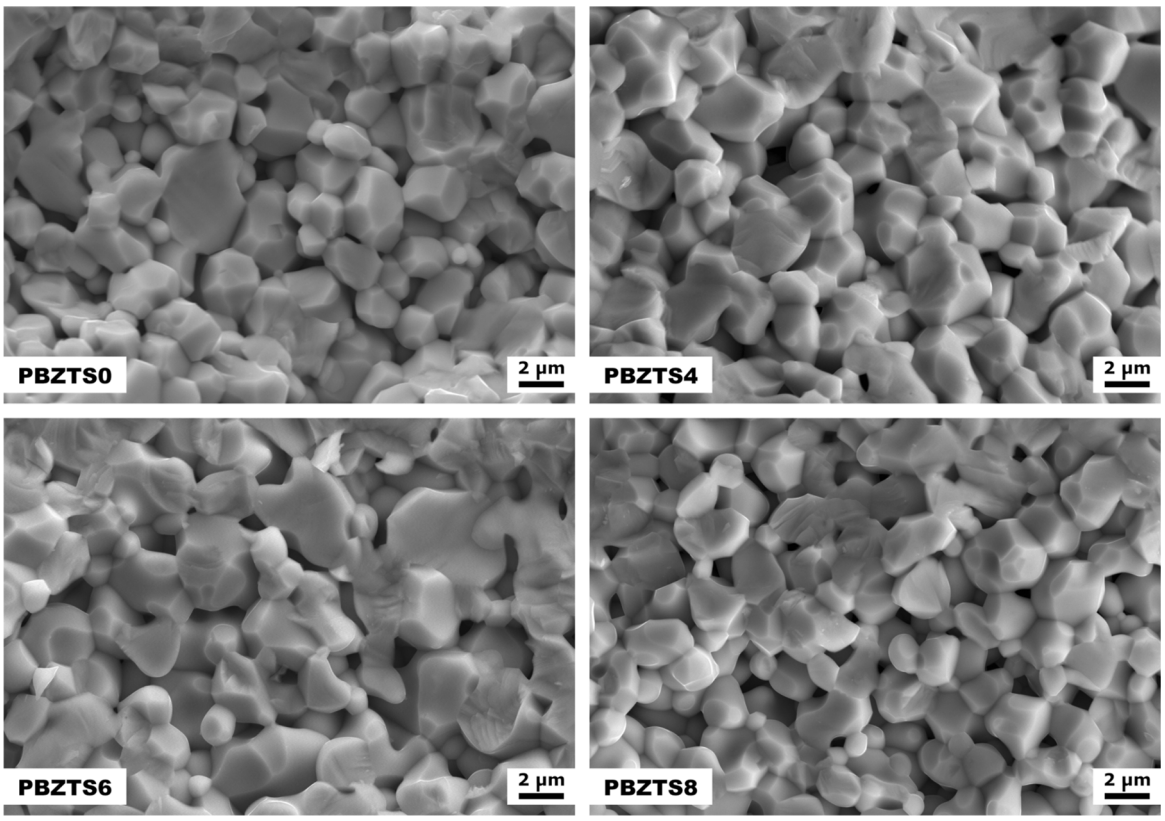

Fig. 2. Microstructure of fractured PBZTS ceramic samples ($z = 0 \div 0.08$)

TABLE 2

The electro-physical parameters of the PBZTS ceramic samples

Abbrev.	ρ [g/cm^3]	$\bar{r}$ [mm]	ε_r [a,b]	tanδ [a,b]	T_m [°C] [b]	ε_m at T_m [b]	tanδ at T_m [b]	E_{a1} [eV] [c]	E_{a2} [eV] [d]
PBZTS0	6.759	1.79	134	0.0364	225	664	0.1393	0.19	0.02
PBZTS4	5.765	2.05	156	0.0272	212	1168	0.1104	0.37	0.02
PBZTS6	6.240	2.02	161	0.0474	203	1536	0.0629	0.40	0.02
PBZTS8	7.014	1.91	166	0.0106	199	3264	0.2727	0.32	0.01

[a] – at room temperature, [b] – at 1 kHz, [c] – at high temperatures, [d] – at low temperatures

studies have shown that Sn-content reduces excessive grain growth, however, their appearance indicates the need to slightly modify (increase) the time or sintering temperature, in order to properly crystallize the appearance of the grains. The average grain size for PBZTS ceramics is from 1.79 to 2.05 μm (Table 2). The linear method (secant) was used to determine the average grain size.

Results of the dielectric investigations of the obtained PBZTS ceramic samples are presented in Figs 3-6. $\varepsilon'(T)$, curves in Fig. 3 exhibit two anomalies probably associated with phase transitions. The first maximum (143-153°C) is associated with ferroelectric orthorhombic-tetragonal phase transition, the second sharper maximum in the range of 199-225°C is linked to phase transformation from the ferroelectric phase in the paraelectric phase (tetragonal-cubic). For 1 kHz, the first transformation occurs in temperatures 143°C, 146°C, 151°C and 153°C for compositions PBZTS0, PBZTS4, PBZTS6, PBZTS8, respectively. There was no clear relation between the value of frequency and the value of the temperature of the maximum of dielectric permittivity. As the frequency of the measuring field increases, a slight decrease in the value of dielectric permittivity throughout the measuring area will be observed. The highest value of dielectric permittivity was observed for PBZTS8 ceramics (see Table 2), which is 3 264 at 199°C (for frequency 1 kHz of the measuring field).

Unified dependencies of $\varepsilon'/\varepsilon'_{max}$ obtained from dielectric measurements were shown in Fig. 4. It can be seen from Fig. 4, that for 1 kHz, with increasing Sn-content, the main maximum of ε' shifts towards lower temperatures, whereas the transformation becomes more sharp. On the other hand, the anomaly associated with the transformation in the range 143-153°C conversely, i.e. with the increase of Sn-content, shifts slightly towards higher temperatures.

Sn addition reduces the value of dielectric loss at room temperature, while at the temperature of phase transition, however, the highest dielectric loss is observed for PBZTS8 ceramics (Fig. 5). A decrease in the tangent value of the angle of dielectric loss can be noticed as the frequency of the measuring field in-

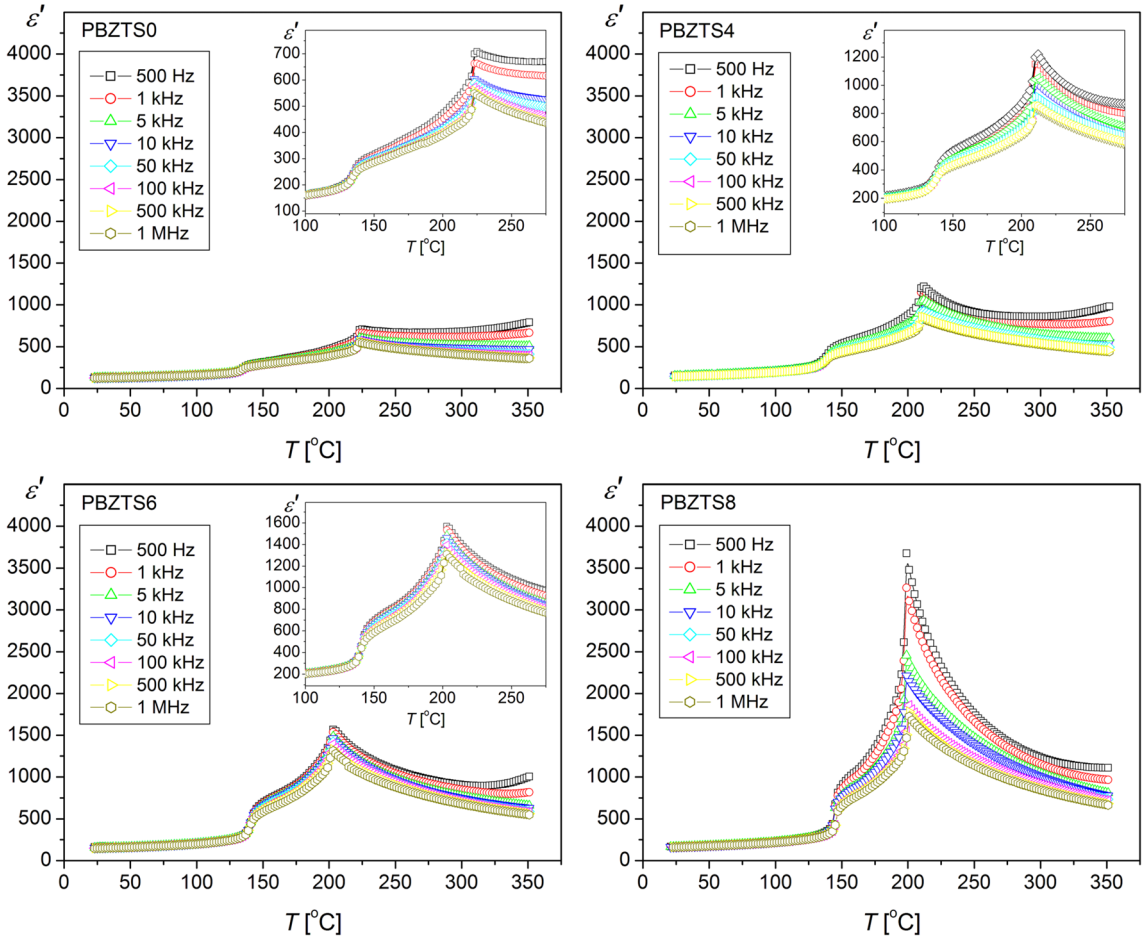

Fig. 3. Temperature dependence of dielectric permittivity of the PBZTS ceramic samples (z = 0÷0.08)

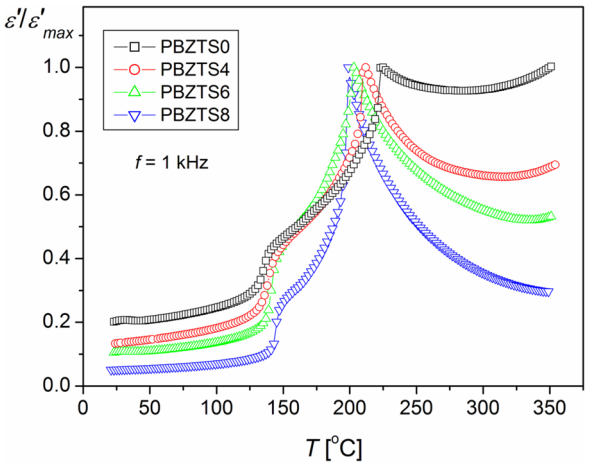

Fig. 4. Unified dependencies of $\varepsilon'/\varepsilon'_{max}$ for PBZTS (z = 0÷0.08), f = 1 kHz

creases. The results of the studies also showed that for ceramics without Sn there is no clear maximum on the temperature course of tan$\delta(T)$ visible to the doped compositions (characteristic of multi-component materials with a perovskite type structure). The electro-physical parameters of the PBZTS ceramic samples are presented in Table 2.

It is seen from Fig. 6 that $\varepsilon'(f)$ for PBZTS x = 0.3, y = 0.2, z = 0÷0.08 slightly decreases with increasing frequency, however no strong anomalies are visible. It is typical for Deby'e relaxation with one time of relaxation.

Results of the calculations of AC electrical conductivity for the analyzed samples are presented in Fig. 7. The results of the AC and DC electrical conductivity tests show that the values of σ_{ac} are higher than the values of σ_{dc}. These values (σ_{ac}) increase with increasing frequency of the measuring field. This is a rather common behaviour for ceramic materials in which the maximum of dielectric permittivity related with phase transition can be observed. Strictly speaking, two maxima are visible in Fig. 7. Based on data from Fig. 7, activation energies at high (E_{a1}) and low temperatures (E_{a2}) have been calculated. These values are shown in Table 2. The introduction of the Sn-addition into the base PBZT composition causes the increase of activation energy at high temperatures from 0.19 eV to approximately 0.36 eV. The activation energy at low temperatures for all PBZTS compositions is about 0.02 eV, and it suggests the existence of a small polaron.

In Fig. 8 the values of σ_{ac} vs. frequency for the PBZTS ceramics tested are shown. Based on these curves, parameter s is calculated. The experimental values of s obtained for all compositions are illustrated in Fig. 9. It is clear from this figure that the parameter s rather decreases with increasing temperature. The data are summarized in Table 3.

The temperature dependence of s provides information to specify the suitable mechanism involved for AC conductivity.

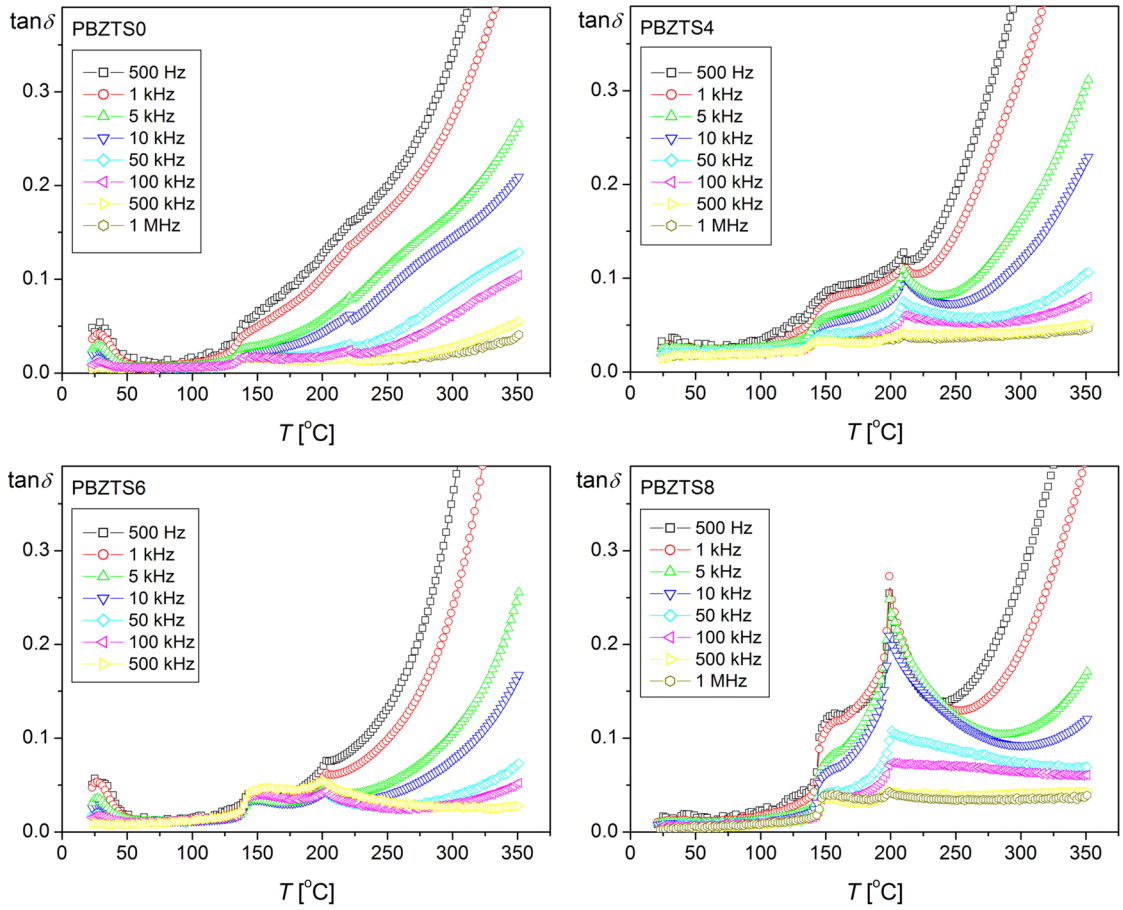

Fig. 5. Temperature dependence of tan$\delta(T)$ for PBZTS ($z = 0 \div 0.08$)

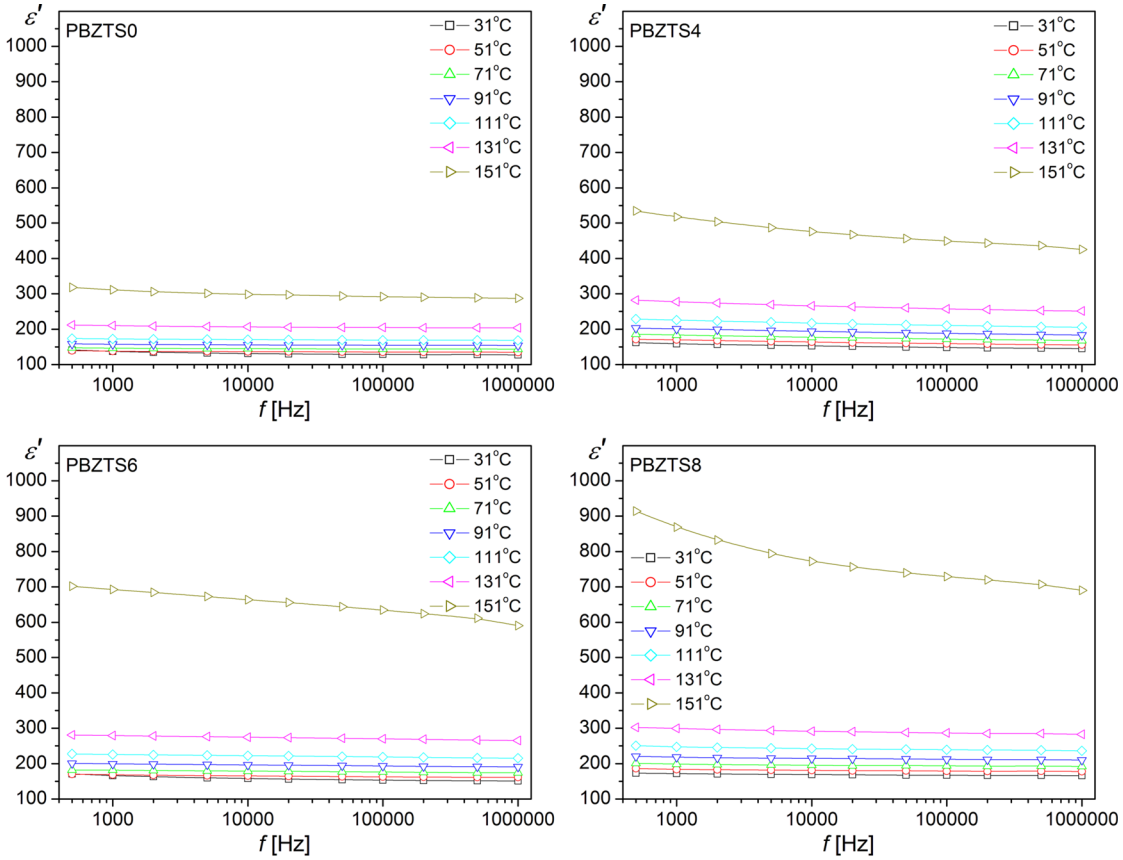

Fig. 6. Frequency dependencies of $\varepsilon'(f)$ for PBZTS ($z = 0 \div 0.08$)

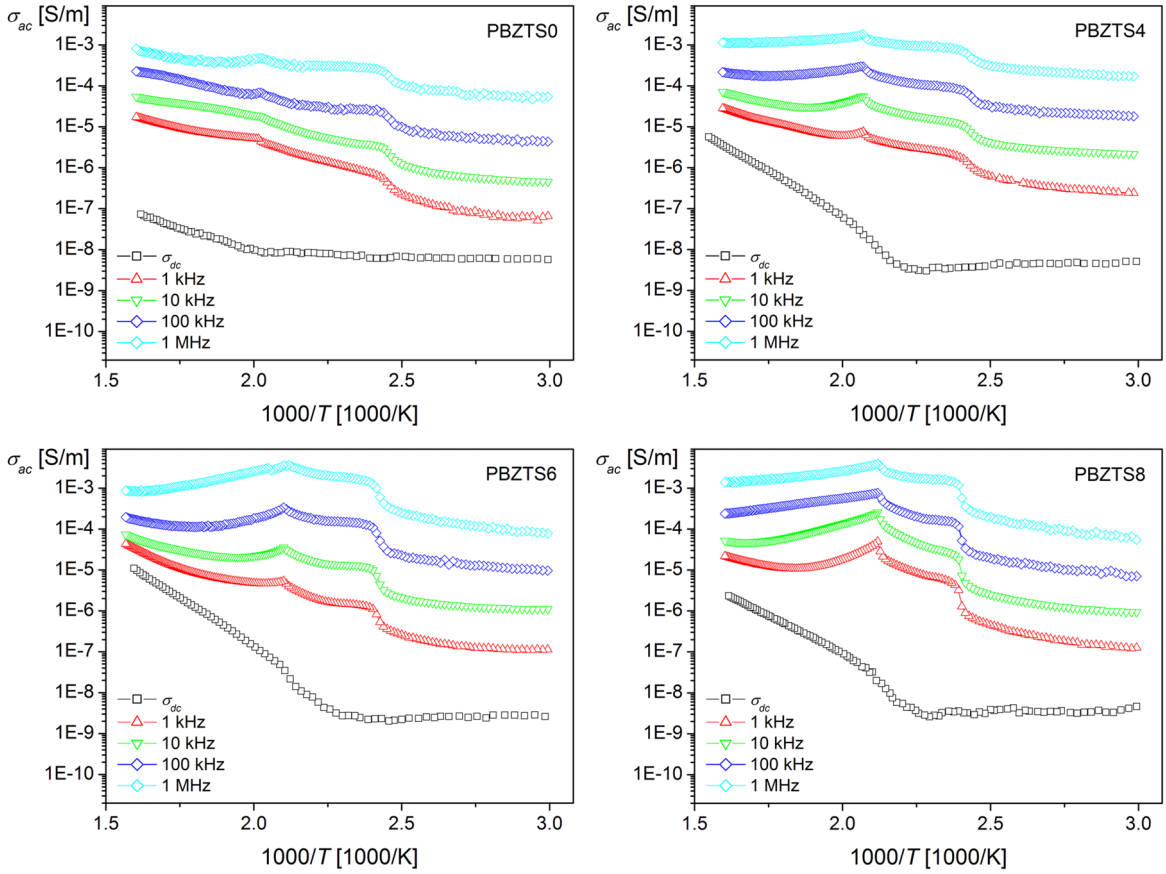

Fig. 7. AC electrical conductivity of the PBZTS ceramic samples (z = 0÷0.08) calculated from formula (1) and compared with DC electrical conductivity measured at 5 V

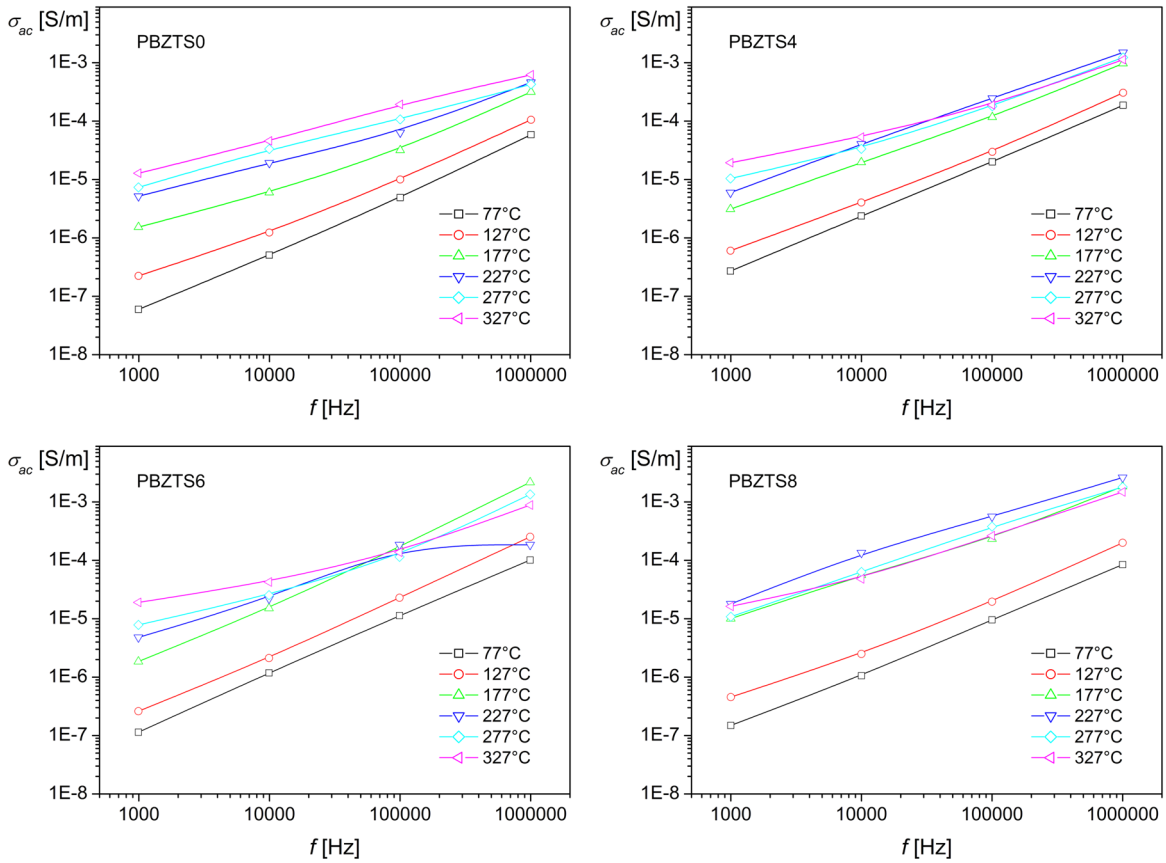

Fig. 8. AC conductivity as a function of frequency for PBZTS ceramics (symbols) and results of fitting to Jonscher's law (lines)

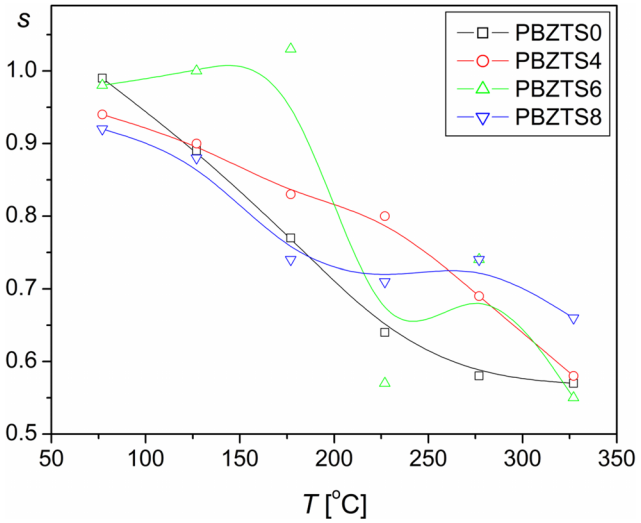

Fig. 9. The $s(T)$ relationships obtained by fitting experimental results to Jonscher's law

TABLE 3

The s-parameters of the PBZTS ceramic samples

T [°C]	s			
	PBZTS0	**PBZTS4**	**PBZTS6**	**PBZTS8**
77	0.99	0.94	0.98	0.92
127	0.89	0.9	1	0.88
177	0.77	0.83	1.03	0.74
227	0.64	0.8	0.57	0.71
277	0.58	0.69	0.74	0.74
327	0.57	0.58	0.55	0.66

This behaviour of AC conductivity is analogous to that observed in ionic glasses [16]. The value of $s = 1$ is regarded theoretically as the limiting value. However, in the latest literature this exponent s is not limited to values below 1 [19-20]. The term $A\omega^s$ can often be explained on the basis of two distinct mechanisms for carrier conduction: quantum mechanical tunneling (QMT) through the barrier separating the localized sites and correlated barrier hopping (CBH) over the same barrier. In these models, the exponent s is found to have two different trends with temperature and frequency. If the AC conductivity is assumed to originate from QMT, s is predicted to be temperature independent, however is expected to show a decreasing trend with ω, while for CBH the value of s should show a decreasing trend with an increase in temperature. The exponent s has been found to behave in a variety of forms [21]. In Fig. 9 it can be seen that s decreases with increasing temperature from 0.99 to 0.57 for the PBZTS0 composition, as well as from 0.92 to 0.66 for the PBZTS8 composition as an example. In the case of PBZTS6 ceramics at a temperature of 177°C, an increase in the value of s above 1 is observed. It may be associated with the appearance of oxygen vacancies. According to Funke [22], the value of the parameter s might have a physical meaning. When $s \leq 1$ would mean that the hopping motion involved is a translational motion with a sudden hopping. However, the value of s greater than 1 would mean that the motion involved is a localized hopping of the species with a small hopping without leaving the neighborhood. The frequency at which a change in slope takes place is known as hopping frequency of the polarons which is temperature dependent.

4. Conclusions

In conclusion, PBZTS ceramic compositions with different amounts of Sn (z = 0-0.08) using conventional ceramic technology were obtained. The results show that the increase in Sn content organizes the microstructure of ceramics, which results in an improvement in the dielectric properties of ceramic samples received (PBZTS8). Analyzing Fig. 3, it can be stated that all graphs $\varepsilon'(T)$ exhibit two anomalies. Probably the anomaly at temperature range 143-153°C can be connected with orthorhombic-tetragonal phase transition, while the second one at temperature range 199-225°C can be connected with tetragonal-cubic phase transition. With increasing Sn-content in the basic composition, the absolute values of $\varepsilon'(T)$ are higher than for $z = 0$ practically at every temperature. For higher addition of Sn the shift of the maximum of ε' towards lower temperatures is observed.

In the case of all samples, the influence of frequency of the measuring field on the temperature (T_m) is not visible. With increasing Sn-content transformation becomes more sharp.

Dependencies of $\tan\delta(T)$ presented in Fig. 5 are more complicated, however the maximum at about 200°C is the most pronounced for PBZTS8. $\varepsilon'(f)$ for PBZTS0÷PBZTS8 slightly decreases with increasing frequency, but there are no strong anomalies visible. Analyzing AC and DC conductivities (Fig. 7), it is seen that the influence of introduction of Sn is rather similar and not big.

The angular frequency dependence of AC conductivity is found to follow universal Jonscher's power law (UDR). The decreases of s-parameter with increasing temperature are similar to those observed in amorphous semiconductors, glasses and crystalline materials. The frequency and temperature dependence of AC conductivity and the small values of activation energy at low temperatures suggest that the hopping conduction is an operating mechanism. The AC component of the frequency dependent conductivity can be expressed as the sum of two different conduction mechanisms, where the first represents the relativity weak temperature dependence, which has been interpreted as being due to hopping of charge carriers, and second represents the strong temperature dependence component [23].

REFERENCES

[1] D. Bochenek, R. Zachariasz, P. Niemiec, J. Ilczuk, J. Bartkowska, D. Brzezińska, Mech. Syst. Sig. Process **78**, 84-90 (2016).

[2] J.A. Bartkowska, J. Magn. Magn. Mater. **374**, 703-706 (2015).

[3] A. Smolenskii, A.I. Agranovskaya, N. Krainik, Dokl. Akad. Nauk SSSR **91**, 55-58 (1953).

[4] M.E. Lines, A.M. Glass, Principles and Applications of Ferroelectrics and Related Materials, Clarendon, Oxford, 1977.
[5] B. Jaffe, W.R. Cook, H. Jaffe, Piezoelectric Ceramics, Academic, New York, 1971, p. 239.
[6] T. Ikeda, J. Phys. Soc. Japan **14**, 168-174 (1959).
[7] G. Li, G.H. Haertling, Ferroelectrics **166**, 31-45 (1995).
[8] A. Amin, R.E. Newnham, L.E. Cross, Phys. Rev. B **34** (3), 1595-1598 (1986).
[9] Z. Ujma, M. Adamczyk, J. Handerek, J. Eur. Ceram. Soc. **18**, 2201-2007 (1998).
[10] J. Handerek, M. Adamczyk, Z. Ujma, Ferroelectrics **233**, 253-270 (1999).
[11] T. Bongkarn, C. Thiangchit, Ferroelectrics **383**, 78-83 (2009).
[12] D. Brzezinska, R. Skulski, P. Wawrzała, G. Dercz, Arch. Metall. Mater. **58**, 1377-1380 (2013).
[13] D. Bochenek, P. Niemiec, R. Skulski, M. Adamczyk, D. Brzezińska, J. Electroceram. **42**, 17-30 (2019).
[14] D. Bochenek, R. Skulski, P. Wawrzała, D. Brzezińska, Ferroelectrics **418**, 82-87 (2011).
[15] R. Skulski, D. Bochenek, P. Wawrzała, G. Dercz, D. Brzezińska, Int. J. Appl. Ceram. Technol. **10** (2), 330-338 (2013).
[16] L. Peng, Yang Tong-Qing, X. Zhuo, Zhang Liang-Ying, Y. Xi, Acta Phys. Sin. **49**, 1852-1857 (2000) (in Chinese).
[17] A.K. Jonscher, Nature **267**, 673-679 (1977).
[18] A.K. Jonscher, J. Mater. Sci. **16**, 2037-2060 (1981).
[19] A.K. Roy, A. Singh, K. Kumari, K. Amar. Nath, A. Prasad, K. Prasad, Adv. Mater. Res. **1** (2), 115-128 (2012).
[20] A.N. Ppapathanassiou, I. Sakellis, J. Grammatikakis, Appl. Phys. Lett. **91**, 122911 (2007).
[21] K. Prasad, Lily, K. Kumari, K.L. Yadav, J. Phys. Chem. Solids **68** (8), 1508-1514 (2007).
[22] K. Funke, Prog. Solid State Chem. **22**, 111-115 (1993).
[23] N.A. Hegab, M.A. Afifi, H.E. Atyia, M.I. Ismael, Acta Phys. Pol. A **119**, 416-423 (2011).